Journal of Engineering and Sustainable Development
Vol. 23, No.01, January 2019
ISSN 2520-0917
https://doi.org/10.31272/jeasd.23.1.4

EXPERIMENTAL STUDY OF SELF-COMPACTING REINFORCED CONTINUOUS DEEP BEAMS

Dr. Adnan Falih Ali [1], * Dr. Abdul_Qader Nihad Noori [2]

1) Prof., Civil Engineering Department, University of Baghdad, Baghdad, Iraq.
2) Lecturer, Civil Engineering Department, Mustansiriyah University, Baghdad, Iraq.

Abstract: Test results of twelve reinforced self-compacted concrete two-span deep beams casted by using self-compacting concrete are reported. The main variables studied were shear span-to-overall depth ratio (a/h), concrete strength (f'c) and the amount of vertical shear reinforcement ratio (ρ_v). All specimens had the same dimensions and main flexural reinforcement. Tests pointed out that all beams failed in shear with diagonal splitting mode. It was found that shear span to overall depth ratio (a/h) effects the load carrying capacity of beams such that a decrease of 50 % in that ratio from 1 to 0.5, the cracking load (P_{cr}) and ultimate load (P_{ult}) increase by average ratios of 29% and 25% respectively. The concrete compressive strength (f'c) are also had a noticeable influence on the continuous deep beams behavior such that increasing (f'c) to almost twice from (33.81 to 6٧.٨) MPa led to an increase in the cracking load (P_{cr}) and ultimate load (P_{ult}) by average ratios of 12.75% and 16.5% respectively. When (ρ_v) is increased by 80% from (0.25% to 0.45%) a better increase shear capacity of both NSCC & HSCC deep beam having (a/h) ratio of 1.0 (enhancement reached to18.56% and 23.1% respectively) as compared to the reference beams without shear reinforcement (ρ_v=0).

Keywords: *continuous deep beam, self-compact concrete, shear span to overall depth ratio, silica fume.*

دراسة عملية على العتبات المسلحة المستمرة العميقة المصبوبة باستخدام الخرسانة ذاتية الرص

الخلاصة: في هذا البحث تم عرض وتحليل النتائج العملية لأثنى عشر نموذج من العتبات العميقة المسلحة المكونة من فضائين والمصبوبة باستخدام الخرسانة ذاتية الرص. المتغيرات الرئيسية التي تم دراستها هي النسبة بين مسافة القص الى العمق الكلي (a/h)، مقاومة الخرسانة (f'c) المسلحة ونسبة حديد القص العمودي (ρ_v). جميع النماذج كانت متساوية من حيث الابعاد و من حيث نسبة حديد التسليح الرئيسي (المقاوم للانثناء). تشير نتائج الفحوصات الى أن جَميع العتبات فشلت بالقص وبإسلوب الإنفصال القُطري. لجميع العتبات وجد أنه بنقصان نسبة (فضاء القص الى العمق الكلي للعتبة) بنسبة ٥٠% من (١.٠ الى ٠.٥) أدى الى زيادة كُلٌ من حمل التشقق والحمل الاقصى للعتبة بمعدل ٢٩% و ٢٥% على التوالي. نتائج الفحوصات العملية تدل على إنه بزيادة مقاومة الإنضغاط الى الضعف على الأغلب من (٣٣.٨١ الى ٦٧.٨ MPa) أدت الى زيادة كل من حمل التشقق والحمل الأقصى بمعدل ١٢.٧٥% و ١٦.5% على التوالي. عند زيادة نسبة تسليح القص الشاقولي من (٠.٢٥% الى ٠.٤٥%) بنسبة تصل الى ٨٠% أدت الى زيادة جيدة في قابلية الحمل الأقصى لكلا النوعين من مقاومة الانضغاط (HSCC & NSCC) للعتبات ذات (a/h=1) (بنسبة وصلت الى ١٨.٥٦% و ٢٣.١% على التوالي) مقارنة بالبلاطة المصدر.

1. Introduction

Reinforced concrete continuous deep beams are fairly common structural elements. They are used in high-rise building as transfer girders, bankers and in folded plates.

*Corresponding Author phd.abdulqadernihad1974@gmail.com

They have the ability to receive receiving many small loads and transferring them to a small number of reaction points [1].

Continuous deep beams act differently from both simply supported deep beams and continuous slender beams. By ignoring these differences through design, one gives up potential available strength and may get significant unpredicted cracking. Continuous deep beams show a distinct 'tied arch' or 'truss' behavior not exist in continuous slender beams. This leads us to an important conclusion that traditional reinforcement detailing rules, based on shallow beams or simply span deep beams are not necessarily suitable for continuous deep beams[2], [3].

Self-compacting concrete is type of concrete that can spread freely into place under its own weight and fill restricted sections as well as jammed reinforcement in structures with no need of mechanical consolidation and without undergoing any significant separation of material constituents[4]. Self-compacting concrete can be considered as special type of concrete, it is different from the traditional concrete in that it has greater flow rate when pumped because of its lower viscosity, also it has no bleeding, no blocking tendency and take a horizontal concrete level after placing[5]. Because of deep beams heavy reinforcement, the difficult of filling areas between congested reinforcement is serious, the conventional concrete does not flow well when it travels to the web and does not completely fill the bottom part. This results in many problems in concrete such as, voids, segregation, weak bond with reinforcement bars and holes in its surface Therefore, self-compacting concrete (SCC) is the suitable choice to be used for those members [5].

There have been many experimental investigations of simply supported reinforced self-compacted concrete deep beams but very few tests are presented on continuous RC deep beams and a few paper[6] till now investigate the behavior of reinforced self-compacted continuous deep beams so this research came to fill the shortage in this area.

2. Experimental Program

Twelve two-span reinforced self-compacted concrete deep beams were tested. All beams had the same span length, width and high. Also, the flexural reinforcement was the same for all beams. Each beam had an overall length of 2300 mm divided by two-spans with 1000 mm for each, a width of 150 mm and a height of 500 mm as shown in Fig. 1 and they were designed to fail in shear. The locations of center lines of loads and supports were the same for all test beams.

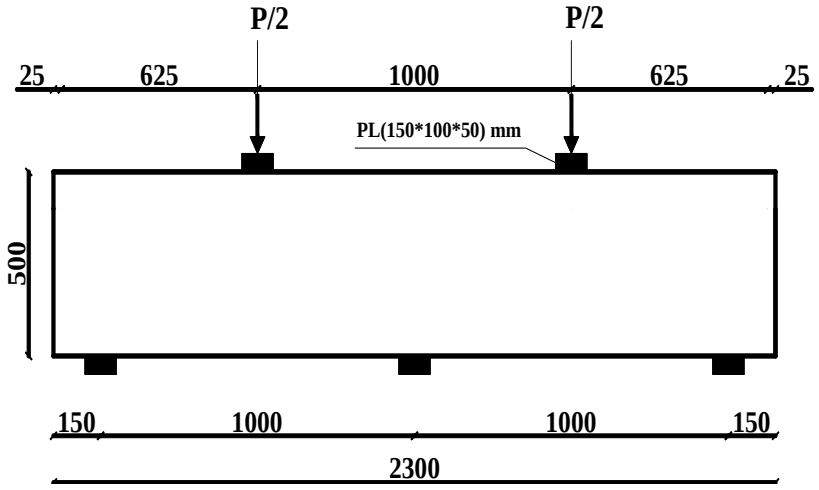

Figure 1. Geometrical Dimensions of the Tested Deep Beams (dimensions in mm)

Specimens are divided into two main groups according to the compressive strength of concrete (NSCC and HSCC) normal and high strength self-compacted concrete respectively, where [NSCC ($f'c < 41$ MPa) and HSCC ($f'c > 41$ MPa)] according to ACI 363R[7].These parameters are chosen according to their importance in determination of SCC continuous deep beams behavior and to fill the shortage in knowledge of behavior of such type of continuous deep beams that constructed using normal strength of SCC. Each group is subdivided into two subgroups according to the ratio of shear span to overall depth ratio (a/h), where (a/h1 = 0.5) and (a/h2 = 1). Moreover, each subgroup consists of three specimens subdivided with respect to the ratio of vertical shear reinforcement (ρ_v) as follow (CDB_A, CDB_B, and CDB_C) where:

The beams with (CDB_A) symbol are refers to the tested specimens without vertical shear reinforcement ($\rho_v = 0$) these specimens considered as reference beams. Beams with (CDB_B) symbol refers to the tested specimens having a minimum vertical shear reinforcement ratio ($\rho_{vmin} = 0.0025$) according to ACI318M-2011[8] provisions. Finally, beams with (CDB_C) symbol refers to tested specimens with maximum vertical shear reinforcement ratio ($\rho_{vmax} = 0.0045$).

The main longitudinal reinforcement at top and bottom was adequate and were kept constant for all tested continuous deep beams to prevent flexural failure. The magnitude of flexural reinforcement (top and bottom) for all the tested beams was the same (4Ø 16mm) with flexural reinforcement ratio equal to ($\rho v = 0.0213$). The vertical shear reinforcement ratio (ρ_v) implemented in (ρ_{vmax}) maximum ratio and (ρ_{vmin}) minimum ratio. For (ρ_{vmax}) maximum Ø8 mm steel bars were used (Ø 8 mm @150 mm c/c) to provide vertical shear reinforcement ratio equals to (0.0045). This percentage of vertical shear reinforcement is larger by about (1.8) times than the minor proportion of vertical shear reinforcement mentioned in ACI318M-2011[8]. To provide minimum vertical shear reinforcement ratio ($\rho_{vmin} = 0.0025$) a Ø6mm steel bars a steel bar with

diameter of (Ø 6mm @150 mm c/c) are used. "Table 1" shows the details of tested beams and research parameters.

All longitudinal bottom steel reinforcement covers full length of the beams and through the depth to provide sufficient anchorage lengths. The vertical web reinforcement was of closed stirrups and the horizontal web reinforcement as longitudinal bars in both sides of the beam.

Specimens were tested in a compression machine with variable monotonic static loads applied at each mid-span and three-quarters of the beam length for (a/h=1.0 and 0.5), respectively. All tested beams were loaded up to failure. Each span has 1000 mm overall clear length (L) which results in a ratio of (L/h=2) that is less than 4.0 as recommended by the ACI318M-2011[8]. provisions for deep beam requirements.

Table 1. Details of tested beams and research parameters

Group	Beam No.	Concrete Type	a/h	Vertical shear reinf.	ρ_v %
A	CDB_{A1}	NSCC	1	0	0
	CDB_{A2}		0.5	0	0
	CDB_{A3}	HSCC	1	0	0
	CDB_{A4}		0.5	0	0
B	CDB_{B1}	NSCC	1	Ø6 mm @ 150mm c/c	0.25
	CDB_{B2}		0.5	Ø6 mm @ 150mm c/c	0.25
	CDB_{B3}	HSCC	1	Ø6 mm @ 150mm c/c	0.25
	CDB_{B4}		0.5	Ø6 mm @ 150mm c/c	0.25
C	CDB_{C1}	NSCC	1	Ø8 mm @ 150mm c/c	0.45
	CDB_{C2}		0.5	Ø8 mm @ 150mm c/c	0.45
	CDB_{C3}	HSCC	1	Ø8 mm @ 150mm c/c	0.45
	CDB_{C4}		0.5	Ø8 mm @ 150mm c/c	0.45

3. Material properties

3.1. Cement

Ordinary Portland cement produced at Northern Cement Factory (Tasluja) was used throughout this investigation, with the requirements of the Iraqi Standard Specification I.Q.S. No.5, 1984[9].

3.2. Fine Aggregate

Natural sand brought from AL-Ukaidher region was used in concrete mixes for this investigation. The fine aggregate had (4.75mm) maximum size with rounded partial shape and smooth texture with fineness modulus of (2.43). The obtained results indicate that, the fine aggregate grading is within the Iraqi Specification No. 45/1984[10].

3.3. Coarse Aggregate

Crushed gravel of maximum size 10 mm brought from Al-Niba'ee region was used which conforms to the Iraqi Specification No.45/1984[10].

3.4. Water

Ordinary tap water was used for both mixing and curing of all concrete specimens used in this investigation. It was free from injurious substances like oil and organic materials.

3.5. Superplasticizer

In this work, the super plasticizer used is known commercially as "GLENIUM51". It is a new generation of modified polycarboxylic ether. It is compatible with all Portland cements that meet recognized international standards. Super plasticized concrete exhibits a large increase in slump without segregation. However, this provides enough period after mixing for casting and finishing the concrete surface.

3.6. Limestone powder (LSP)

This material is locally named "Al-Gubra". It is a white grinding material from lime-stones excavated from Al-Mosul province in the north of Iraq, Particle size of the limestone powder is less than 0.125 mm, it is confirm to EFNARC 2002[11].

3.7. Silica fume

The silica fume that was used in present experimental work Equipped by sika[12] Chemical Company, Formerly known as Meyco® MS 610. The chemical composition of the Silica fume is conforming to EN 13263.

3.8. Steel Reinforcing Bars

All reinforcement bars were deformed bars; three types of deformed steel bars according to nominal diameter have been used in this study. Steel bars of nominal diameter of (16) mm were used as longitudinal reinforcement in the tension zone at top and bottom of the beams. Steel bars of nominal diameter of (6) mm were used as stirrups (as minimum ratio) and as horizontal web reinforcement. Finally, steel bars of nominal diameter of (8) mm were used as stirrups (as maximum ratio). According to ASTM C370-05a 2005[13], tensile tests were carried out for the steel reinforcement using three 450 mm long specimens for each nominal diameter. Tensile tests of steel reinforcement are carried out at the laboratory of Materials at the College of Engineering in Mustansiriyah University to determine the average yield stress and the ultimate stress.

The test results are listed in Table 2. Fig. (2-a) to Fig. (2-c) shows the details of reinforcement for each group.

Table 2. Properties of reinforcing steel bars

Nominal bar diameter (mm)	Measured bar diameter (mm)	Bar area (mm^2)	Yield stress (MPa)	Ultimate stress (MPa)	Elongation %
16	16.1	201	495	720	11.3
8	8.02	50.8	431	695	12.8
6	6.08	28.3	570	812	2.7

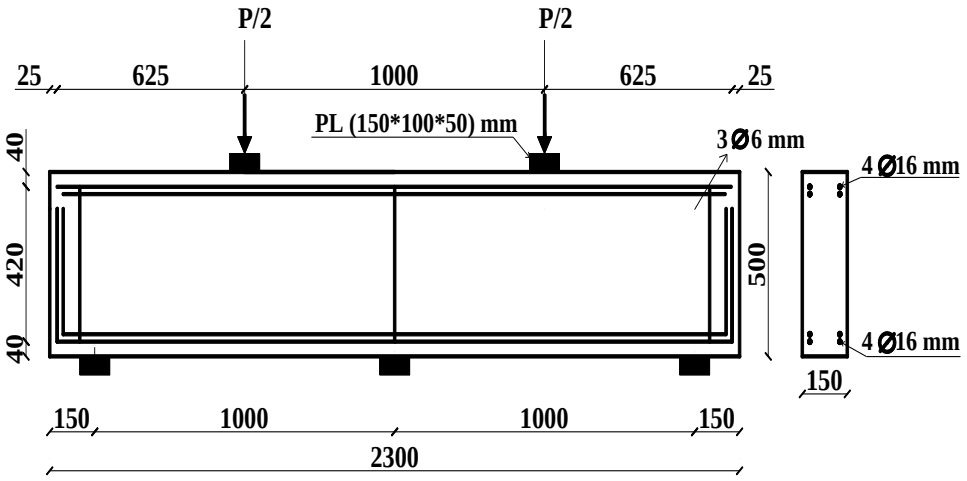

Figure (2-a). Details of beams in group A (all dimensions in mm)

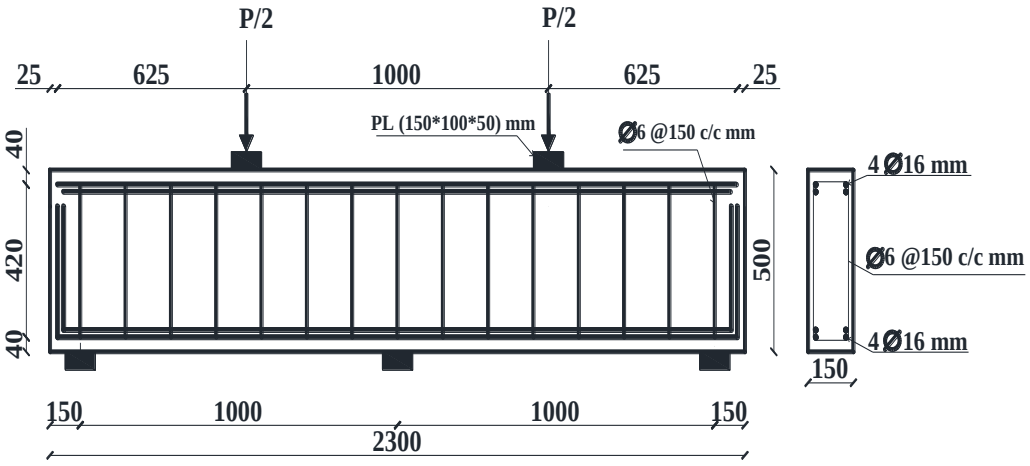

Figure (2-b). Details of beams in group B (all dimensions in mm)

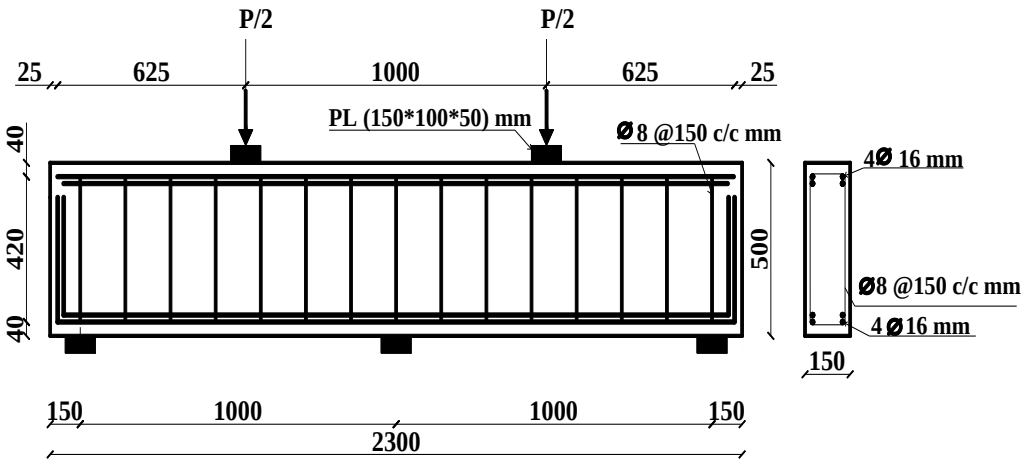

Figure (2-c). Details of beams in group C (all dimensions in mm)

4. Concrete Mix Proportions

To achieve SCC fresh properties the mix was designed according to EFNARC 2002[11]. Regrettably, the fresh properties of SCC are most important than the compressive strength in all mix design methods. In this study, many trial mixes were carried on to obtain the proper design for compressive strength and to achieve the fresh properties of SCC requests commonly. In the present work, the cement content was 400 kg/m3, fine aggregate content was 785 kg/m^3, course aggregate content was 770 kg/m^3, limestone powder contents was 50 kg/m^3, water content was 165 l/ m^3 and the superplasticizer content was 7.5 l/m^3, these values satisfy all the values recommended by EFNARC's mix design method.

5. Mixing Procedure for SCC

The mixing procedure adopted in the laboratory and used in the current study was summarized by Emborg [14] and improved by Al-Jabri [15]. The method is stated as follows:

1. Fine aggregates was added to the mixer and mixed with one third of the total water and mixed for one minute.
2. The cement and mineral admixtures were added at another one-third of water and mixed for one minute.
3. Coarse aggregate was added to the remaining one-third of water and (1/3) dosage of superplasticizer, and the mixing time lasts for (1½) minutes then the mixer continuous for (1/2) minute.
4. Then, the (2/3) of the remaining superplasticizer was added and mixed for (1½) minutes.
5. The concrete was then discharged, tested for fresh properties and cast.

6. Tests on Fresh Concrete Testing Procedure

In this work, consideration of concrete mix as a self-compacting concrete (SCC) is verified by three standard tests: Slump flow, $T_{50\ cm}$ slump flow and L-box, Table 3 show the results of properties of fresh SCC.

Table 3. Tests results of properties of fresh SCC

Mix name	Slump flow, (mm)	T_{50} (sec)	L – box,(H_2/H_1)
NSCC	753	2.5	1
HSCC	714	4.3	0.90
Limits of EFNARC[11]	650-800	2-5	0.8-1
Limits of ACI-237[16]	450-760	2-5	0.8-1

Figure (3-a). Flowing of concrete in horizontal section in L-box test of SCC.

Figure (3-b) Spreading concrete in Slump Flow test of SCC.

From the table above, it is clear that the test results of all mixtures were satisfying the requirements of both the EFNARC [11] and ACI-237R07 [16] limitations.

Moreover, from the values shown in the table above it can be noticed that the value of two tests, slump flow and L-box for HSCC are lower than those of NSCC, while the value of (T_{50}) test for HSCC mix is higher than those of NSCC mix. This means that the workability of HSCC mix is less than workability of NSCC mix, in other meaning, the workability decreases with an increase in the compressive strength. The reason is due to using larger amounts of cement and lower amount of water.

7. Testing Procedure

Initially, all continuous deep beam (CDB) specimens were painted with white at both sides to observe the formation of first crack, crack patterns and the development of these cracks. Thereafter, the beams were labeled then for accuracy; signs were placed to indicate the supports points, loading points, dial gauges and concrete strain gauges

locations. Then the specimens were lifted and placed onto supports to carry out load tests.

All CDB specimens two spans and tested up to failure by applying two symmetrical concentrated loads vertically at the top side of each specimen. the rigid frame helps to divided the single load created by the testing machine into two equal concentrated loads, as shown in Fig. 4.Testing starts by applying the load monotonically in increments of about (10 kN) per stage until failure. Five steel plates each of dimensions of (150x100x50) mm were used as bearing plates located under load and over supports to prevent premature failure or local failure of concrete.

At each loading stage, the strains in steel reinforcement and at concrete surface were recorded and automatically saved by data logger. The crack patterns, dial gauges and the corresponding loads were marked at each load stage. Fig.4 shows the setup of continuous deep beam (CDB).

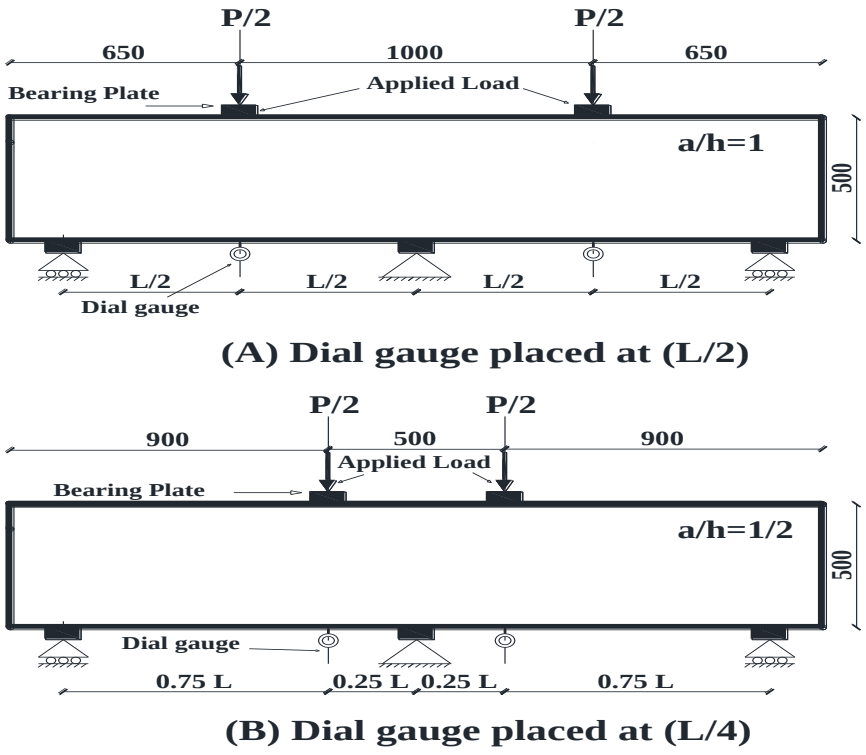

Figure 4. Setup of continuous deep beam (CDB) (all dimensions in mm)

8. Hardened SCC Mechanical Properties Results

The hardened mechanical properties of SCC that were studied in the present work are; concrete compressive strength (f'_c), splitting tensile strength (f_t), modulus of rupture (fr) and modulus of elasticity (Ec). "Table 4" illustrates the test results of the hardened SCC, with the note that each value presented in this table denotes the average value of three specimens.

Table 4. Tests results of mechanical properties for hardened SCC

Group	Beam No.	a/h	f′c (MPa)	f_t (MPa)	f_r (MPa)	Ec (MPa)
A	CDB_{A1}	1	33.81	3.18	4.45	24973.96
	CDB_{A2}	0.5				
	CDB_{A3}	1	66.4	4.48	6.11	٣٣٠٣٢.٧١
	CDB_{A4}	0.5				
B	CDB_{B1}	1	34.52	3.27	4.79	25598.66
	CDB_{B2}	0.5				
	CDB_{B3}	1	66.72	4.53	6.23	33450.54
	CDB_{B4}	0.5				
C	CDB_{C1}	1	36.05	3.41	5.39	26168.40
	CDB_{C2}	0.5				
	CDB_{C3}	1	67.8	4.62	6.63	34418.50
	CDB_{C4}	0.5				

9. Test Results of SCC Continuous Deep Beams

Among all of the tested specimens, it was noted that in general, the first crack was at mid-span developed suddenly in the flexural sagging region just about (20 to 23) % of the ultimate load, after that, the first diagonal cracks starts suddenly at mid-depth of the concrete strut within the interior shear span between the applied load and the middle support.

As observed, the first flexural crack over the middle support occurred at about 80% of the ultimate load. As the load increases, more flexural and diagonal cracks start to develop and a major diagonal crack extended to join the edges of the applied load and the middle support plates.

As the load was increased further, the cracks became wider associated with a large increase of deflection. When the load levels became close to failure loads, the two spans showed nearly the same crack patterns. Finally, at failure, an end block formed because of the significant diagonal crack connecting the edges of the load and the inner support plates, rotated about the end support leaving the rest of the beam fixed over the other two supports. The shear cracking loads at various stages of loadings are shown in Table 5 and in Fig. 5 to Fig.16.

Table 5. Summary of test results for the tested beams

Beam No.	Concrete type	f'c MPa	a/h	a/d	ρ_v%	ρ_h%	P_{cr} (kN)	P_{ult} (kN)	Type of Failure
CDB_{A1}	NSCC	33.81	1	1.25	0.0	0.0	200	873	D.S*
CDB_{A2}			0.5	0.625	0.0	0.0	245	1115	D.S
CDB_{A3}	HSCC	66.4	1	1.25	0.0	0.0	215	992	D.S
CDB_{A4}			0.5	0.625	0.0	0.0	260	1288	D.S
CDB_{B1}	NSCC	34.52	1	1.25	0.25	0.0	205	958	D.S
CDB_{B2}			0.5	0.625	0.25	0.0	265	1180	D.S
CDB_{B3}	HSCC	66.72	1	1.25	0.25	0.0	230	1120	D.S
CDB_{B4}			0.5	0.625	0.25	0.0	310	1407	D.S
CDB_{C1}	NSCC	36.05	1	1.25	0.45	0.0	220	1035	D.S
CDB_{C2}			0.5	0.625	0.45	0.0	280	1277	D.S
CDB_{C3}	HSCC	67.8	1	1.25	0.45	0.0	247	1221	D.S
CDB_{C4}			0.5	0.625	0.45	0.0	340	1480	D.S

* D.S = Diagonal Splitting.

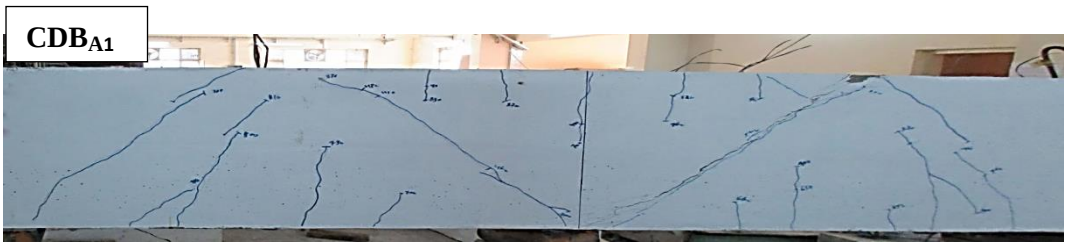

Figure 5. Crack pattern for beam CDB_{A1} after testing

Figure 6. Crack pattern for beam CDB_{A2} after testing

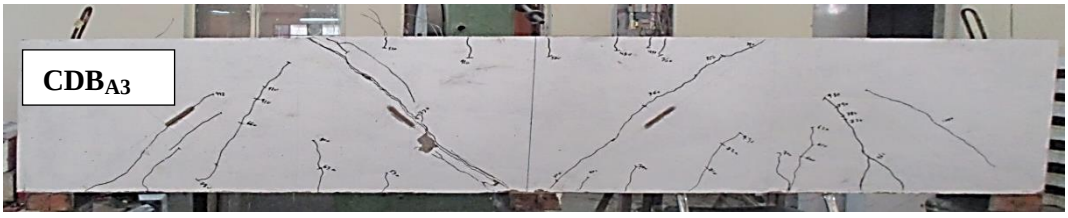

Figure 7. Crack pattern for beam CDB_{A3} after testing

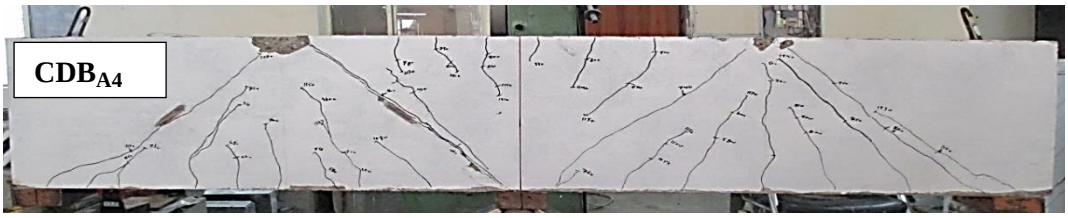

Figure 8. Crack pattern for beam CDB_{A4} after testing

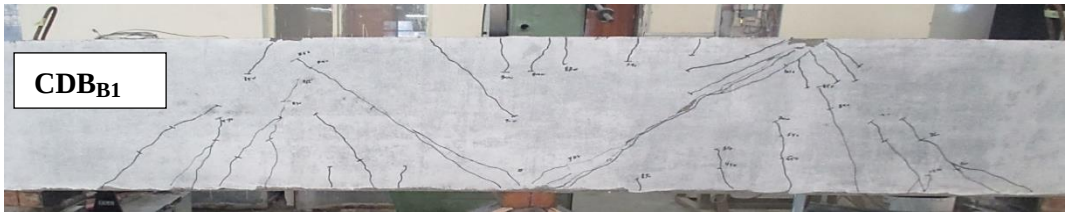

Figure 9. Crack pattern for beam CDB_{B1} after testing

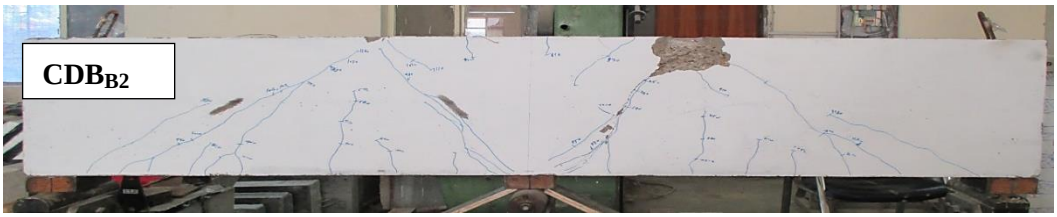

Figure 10. Crack pattern for beam CDB_{B2} after testing

Figure 11. Crack pattern for beam CDB_{B3} after testing

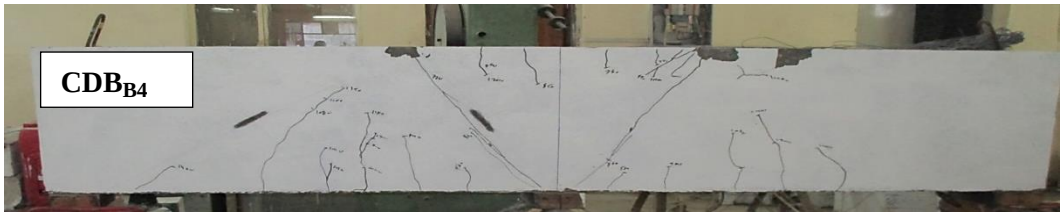

Figure 12. Crack pattern for beam CDB_{B4} after testing

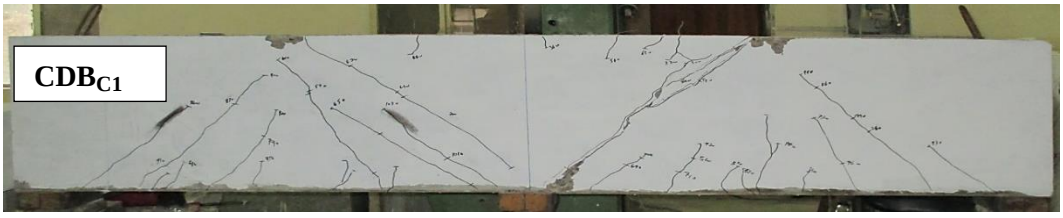

Figure 13. Crack pattern for beam CDB_{C1} after testing

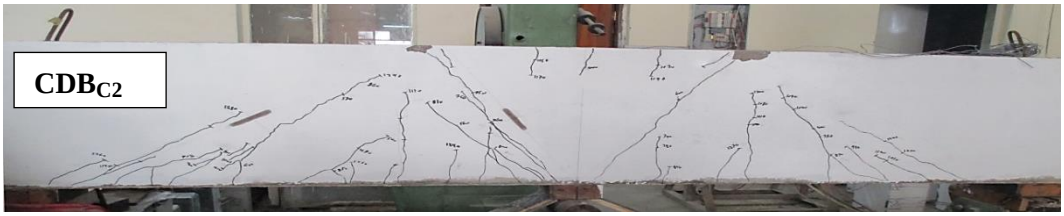

Figure 14. Crack pattern for beam CDB_{C2} after testing

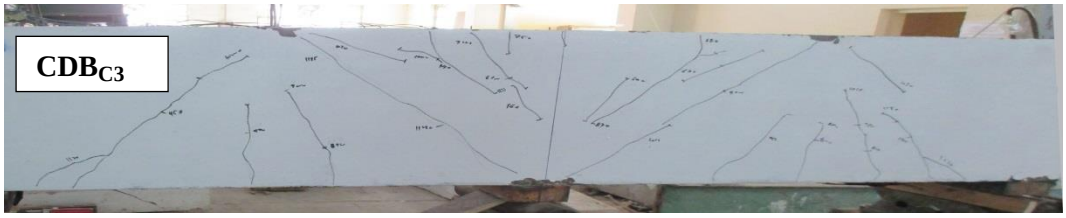

Figure 15. Crack pattern for beam CDB_{C3} after testing

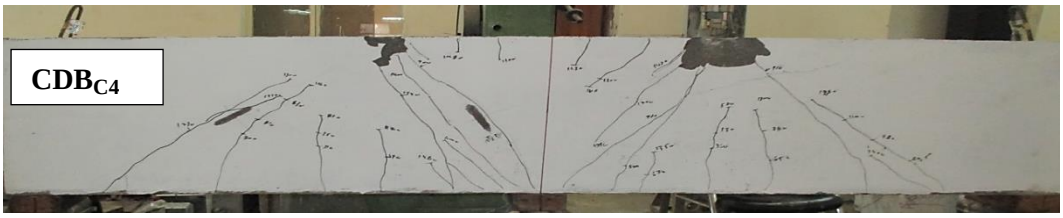

Figure 16. Crack pattern for beam CDB_{C4} after testing

10. Effect of (a/h) Ratio

Generally, for all cases of tested beams of normal or high strength, with or with no vertical or horizontal shear reinforcement, as the ratio of a/h decreases, the ultimate load at failure and first shear cracking load values will increase as shown in Table 5 above. The effect of (a/h) on both ultimate load at failure and first shear cracking load values can be summarized as follows:-

Beams of NSCC, When the ratio of (a/h) decreases by 50% from (1 to 0.5), the ultimate load (P_{ult}) increases according to the type and magnitude of shear reinforcement, (P_{ult}) was found to increase at percentage of (23.4% to 27.7%), that is, increases by an average of about 18.4%, While the first crack load (P_{cr}) increases by percentages of (22.5 to 29.3) %, that is, an average of about 30.2 %. "Table 6" shows the effect of variation of (a/h) ratio on both failure load (P_{ult}) and first cracking load (P_{cr}), respectively.

At the same time, for continuous deep beams casts in HSCC, a reduction in the (a/h) ratio of 50% from (1 to 0.5) results in an increase in the first cracking load by an average value of about 32.3%, for all cases of tested beams with the note that a beam with shear reinforcement shows a better enhancement in (P_{cr}) as compared to the beam with no shear reinforcement (average enhancement of 38.4% vs 20.9%). Moreover, for the same reduction in (a/h) ratio, the ultimate failure load increases by an average of

25.5% with the note that plain concrete beam enhanced by about 29.8% , while beams with shear reinforcement enhanced by an average of 23.4%.

Table 6. variation of first cracking load and ultimate load with the variation of (a/h) ratio

Concrete type	Beam groups	ρ_v%	a/h=1			a/h=0.5			% Variation in loads with (a/h) ratio	
			P_{cr} (KN)	P_{ult} (KN)	p_{cr}/p_{ult} %	P_{cr} (KN)	P_{ult} (KN)	P_{cr}/P_{ult} %	ΔP_{cr} %	ΔP_{ult} %
NSCC	A	0	200	873	22.9	245	1115	22.0	22.5	27.7
	B	0.25	205	958	21.4	265	1180	22.5	29.3	23.2
	C	0.45	220	1035	21.3	280	1277	21.9	27.3	23.4
HSCC	A	0	215	992	21.7	260	1288	20.2	20.9	29.8
	B	0.25	230	1120	20.5	310	1407	22.0	38.4	25.6
	C	0.45	247	1221	20.2	340	1480	23.0	37.7	21.2
Average value					21.33			21.93	29.35	25.15

11. Effect of Concrete Compressive Strength

Two types of self-compacting concrete were adopted in this study, normal compressive strength (NSCC) with f'c ranging between (33.81 to 36.05) MPa and high compressive strength (HSCC) with f'c ranging between (66.4 to 67.8) MPa. The increase in compressive strength of concrete is reflected positively with the not that (P_{ult}) is found to be more sensitive to the variation of f'c than (P_{cr}) in case of (a/h=1.0).

It can be notice that increasing the compressive strength of concrete to almost twice led to an increase in the cracking load by about 6.12% to 21.43% (an average of 12.75%), while the ultimate load was enhanced by 13.63% to 19.24% (an average of 16.53%). Table 7 shows the effect of variation of concrete compressive strength (f'c) on both failure load (P_{ult}) and first cracking load (P_{cr}), respectively.

An increase in the concrete compressive strength (doubling) results in an increase in the values of (P_{cr}) by an average of 14.8% when (a/h=0.5) and by about 10.7% only when (a/h=1) while the increase in values of ultimate load (P_{ult}) was about (16.2% to 16.9%) for both values of (a/h) ratios (0.5 &1.0) respectively.

Table 7. Variation of (P_{cr}) & (P_{ult}) with variation of concrete compressive strength (f'c)

a/h ratio	ρ_v%	Beam group	NSCC			HSCC			%Variation due to increasing (fc)	
			P_{cr} (kN)	P_{ult} (kN)	P_{cr}/P_{ult} (%)	P_{cr} (kN)	P_{ult} (kN)	P_{cr}/P_{ult} (%)	%increase in P_{cr}	%increase in P_{ult}
a/h=1	0.00	A	200	873	22.9	215	992	21.7	7.50	13.63
	0.25	B	205	958	21.4	230	1120	20.5	12.20	16.91
	0.45	C	220	1035	21.3	247	1221	20.2	12.27	17.97
a/h=0.5	0.00	A	245	1115	22.0	260	1288	20.2	6.12	15.52
	0.25	B	265	1180	22.5	310	1407	22.0	16.98	19.24
	0.45	C	280	1277	21.9	340	1480	23.0	21.43	15.9
Average value					22			21.3	12.75	16.53

12. Effect of Vertical Web Reinforcement

To allow for a better understanding of the behavior of deep beams with shear reinforcement, different percentages of web reinforcement were tried and first cracking and ultimate failure loads were recorded for different ratios of vertical reinforcements. "Tables 8" shows the effect of vertical web reinforcement on P_{cr} and P_{ult} load.

It is clear that; presence of web reinforcement (ρ_v) enhances the behavior of continuous deep beams (SCC) by increasing cracking and ultimate loads. A SCC deep beam with 0.25% of (ρ_v) results in an increase in the value of (P_{cr}) by 8.16% to 2.5% for NSCC (a/h= 0.5 &1.0, respectively) while the increase in (P_{cr}) was 19.23% to 7% for HSCC (a/h= 0.5 &1.0, respectively.

The ultimate load carrying capacity (P_{ult}) increases by 5.8% to 9.7 % for the case of NSCC (a/h= 0.5 &1.0, respectively) and by 9.24% to 12.9% for the case of HSCC (a/h= 0.5 &1.0, respectively). This means that two factors have noticeable effects on the shear capacity of a continuous deep beams cast in SCC, that is, ρv and (a/h) ratio as shown in Table 8.

Increasing the magnitude of (ρv) by 80% (from 0.25% to 0.45%) that is (ρv_{min} &ρv_{max}) results in a better increase in the shear capacity of both NSCC & HSCC deep beam having (a/h) ratio of 1.0 (enhancement reached to18.56% and 23.1% respectively) while in case of (a/h) ratio of 0.5, it seems that deep beams cast in NSCC show good enhancement in ultimate load capacity (by 14.53%) while only 14.91% enhancement was noticed in beams cast in HSCC for the same (a/h) ratio of (0.5). As a summary, both serviceability and strength show noticeable enhancement when web reinforcement is implemented and increased further.

Table 8. Effect of vertical shear reinforcement ratio on cracking and ultimate failure loads

Beam No.	Concrete type	a/h	ρ_v%	P_{cr} (KN)	$P_{ult.}$ (KN)	% of increase in P_{cr} comparing with reference beam	% of increase in P_{ult} comparing with reference beam
CDBA1	NSCC	1.00	0.00	200	873	Reference	Reference
CDBB1			0.25	205	958	2.5	9.74
CDBC1			0.45	220	1035	10	18.56
CDBA2		0.50	0.00	245	1115	Reference	Reference
CDBB2			0.25	265	1180	8.16	5.83
CDBC2			0.45	280	1277	5.7	14.53
CDBA3	HSCC	1.00	0.00	215	992	Reference	Reference
CDBB3			0.25	230	1120	7	12.9
CDBC3			0.45	247	1221	14.88	23.1
CDBA4		0.50	0.00	260	1288	Reference	Reference
CDBB4			0.25	310	1407	19.23	9.24
CDBC4			0.45	340	1480	30.77	14.91

13. Load- deflection Relation

The mid-span deflections curves for all the tested beams of each group as a function of the total applied loads are shown in Fig.17 to Fig.19 , they are essential for describing the behavior of a beam at various stages of loading. Those mid-span deflection curves are those recorded at the failed span. At low load level and prior to first crack formation (up to first crack load), the load-deflection relations seem to be linear with semi constant slope. After cracking, the load- deflection response takes a nonlinear form with a variable slope where the deflection increases at an increasing rate as the applied load increases.

The initial stiffness of the tested beams increases with the increase of concrete compressive strength and a decrease in the (a/h) ratio. The flexural cracks that are developed in the sagging zone have little influence on the beam stiffness however larger influence occurs when diagonal cracks in the interior shear span occur.

Increasing shear span to overall depth ratio (a/h) from 0.5 to 1 leads to an increase in deflection values at each stage of loading, the increase in a/h ratio increases bending moment, which causes an increase in the deflection value of CDB.

The load- mid span deflection curves appeared to be strongly dependent on the a/h ratio, magnitude and arrangement of web reinforcement. Fig.18 to Fig.20 show the effect of increasing (a/h) from 0.5 to 1.0 ratio on deflection curves for all three groups

(A, B and C) for NSCC and HSCC beams. For all groups, it is clear that the deflection for NSCC beams is larger than beams of HSCC for the same load level.

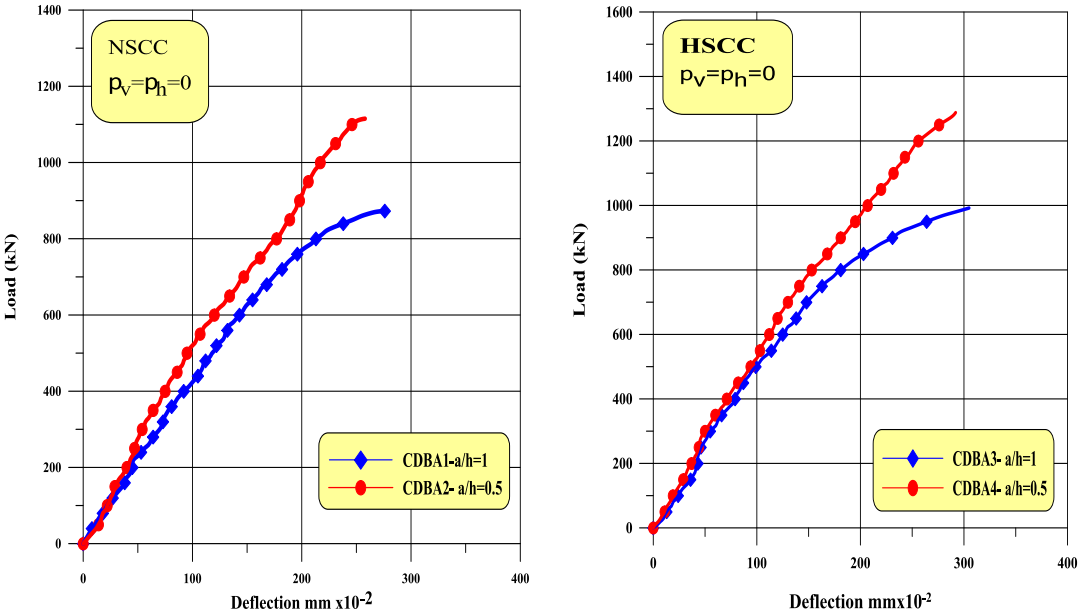

a. Load deflection relationship of NSCC. b. Load deflection relationship of HSCC.

Figure 17. Effect of increasing in a/h ratio on load- midspan deflection response for group (A)

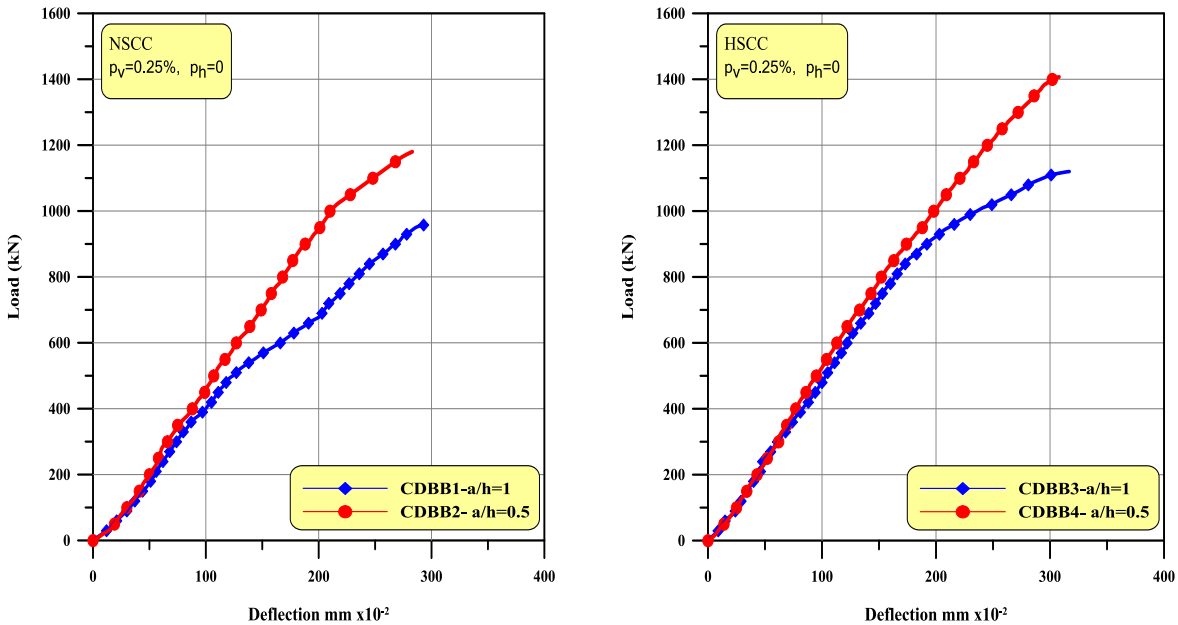

a. Load deflection relationship of NSCC. b. Load deflection relationship of HSCC.

Figure 18. Effect of increasing in a/h ratio on load- midspan deflection response for group (B)

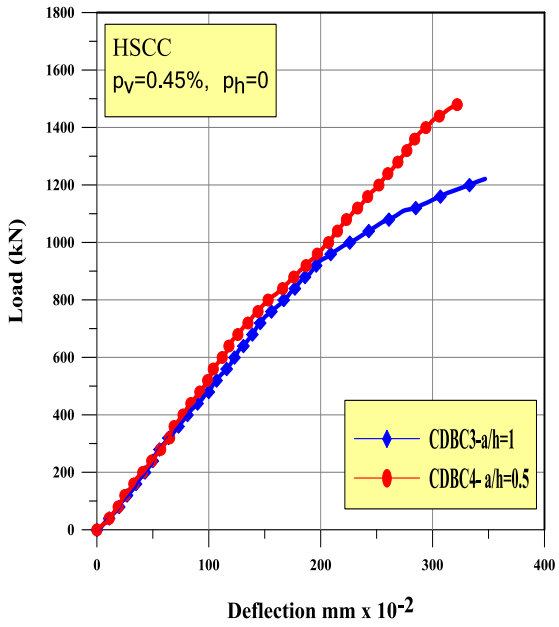

a. Load deflection relationship of NSCC.

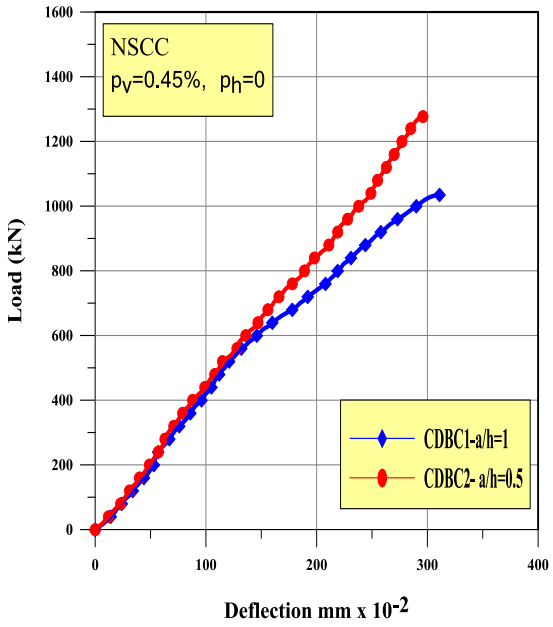

b. Load deflection relationship of HSCC.

Figure 19. Effect of increasing in a/h ratio on load- midspan deflection response for group (C)

for all groups, an increase in compressive strength (f'_c) from (33 to 66)MPa lead to a decrease in deflection values, this reduction can be related to the increases of the flexural rigidity (EI) which reduces the deflection for the same load level. Therefore, the deflection values of HSCC beams are always less than deflection values of NSCC beams for all stages of loading.

Increasing the shear reinforcement improves the shear capacity because of the contribution of this reinforcement with concrete in resisting the diagonal tension stresses which often govern the failure where the reinforcement carries a portion of these stresses. Therefore, increasing the reinforcement area within the shear span leads to delay failure by splitting until it reaches the maximum tension capacity at further loads.

14. Concrete Surface Strains

Concrete strains were measured at critical locations on the tested beams. Two Electrical resistance strain gauges (Type: TML/ PL-60-11-3L) were placed on the front face of the specimen to measure the compressive concrete surface strains, were located at the center of inclined strut track and parallel to the direction of concrete strut, as shown in Fig. 20.

The main objectives of using the concrete strain measurements were to obtain an idea regarding the maximum surface concrete compressive strains for different values of variables such as (a/h) ratio and presence or absence of vertical (with different ratios) shear reinforcement, also to indicate the formation of the first shear crack.

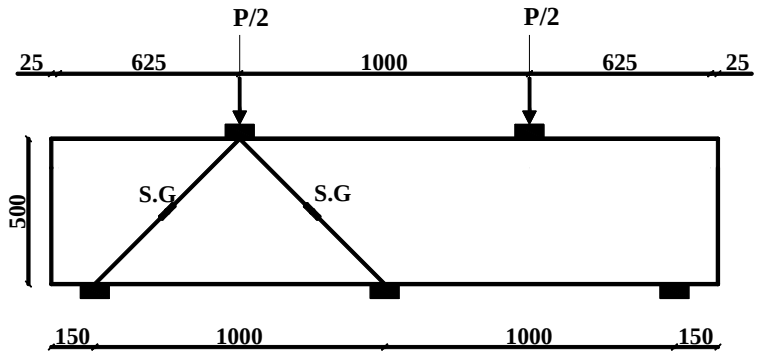

Figure 20. Location of Concrete Strain Gauges on the tested Continuous deep beams (dimensions in mm)

At early stages of loading, the developed concrete surface strains were very small. Further by increasing the applied load a sudden change in the average strain values will occur as shown in Fig. 21 to Fig. 23, at this stage of loading, the formation of first shear crack took place. After that, concrete cracking became visible and strains increased at an increasing rate with respect to the applied load. Table 9 shows the results of the estimated from experimental strain diagram first shear cracking load and the visually observed shear cracking load.

Table 9. Values of experimental shear cracking loads and shear cracking loads obtained from strain diagram

Group No.	Beam No.	P_{cr} (kN) experimental	P_{ult} (kN)	(P_{cr}/P_{ult}) %	P_{cr} (kN) Estimated from Strain diagram	(P_{cr}/P_{ult}) %
A	CDBA1	200	873	23	200	23
	CDBA2	245	1115	22	240	22
	CDBA3	215	992	22	210	21
	CDBA4	260	1288	20	265	21
B	CDBB1	205	958	21	200	21
	CDBB2	265	1180	22	260	22
	CDBB3	230	1120	21	230	21
	CDBB4	310	1407	22	320	23
C	CDBC1	220	1035	21	210	20
	CDBC2	280	1277	22	270	21
	CDBC3	247	1221	20	250	20
	CDBC4	340	1480	23	330	22

After cracking, the load- deflection response takes a nonlinear form with a variable slope where the deflection increases at an increasing rate as the applied load increases. From Table 9 the results are relatively close and the difference in the results may be

explained on the basis that the concrete strain gauges can predict the formation of crack in a manner greatly more accurate than visual inspection.

The average strain diagrams appear to depend on the a/d ratio and amount and arrangement of web reinforcement, the concrete surface compressive strain values increased as the ratio of (a/h) increased from 0.5 to 1.0 as shown in figures above. Moreover, increasing the compressive strain of concrete from NSCC to HSCC led to increasing in the concrete surface compressive strain.

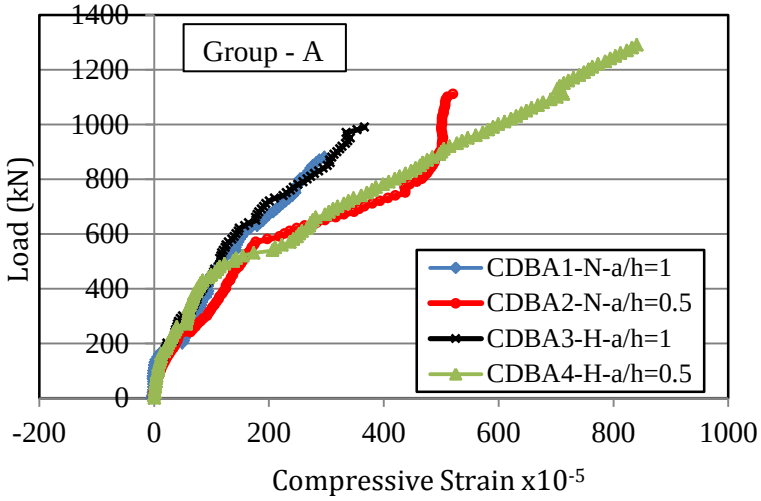

Figure 21. The concrete surface compressive strain in group (A)

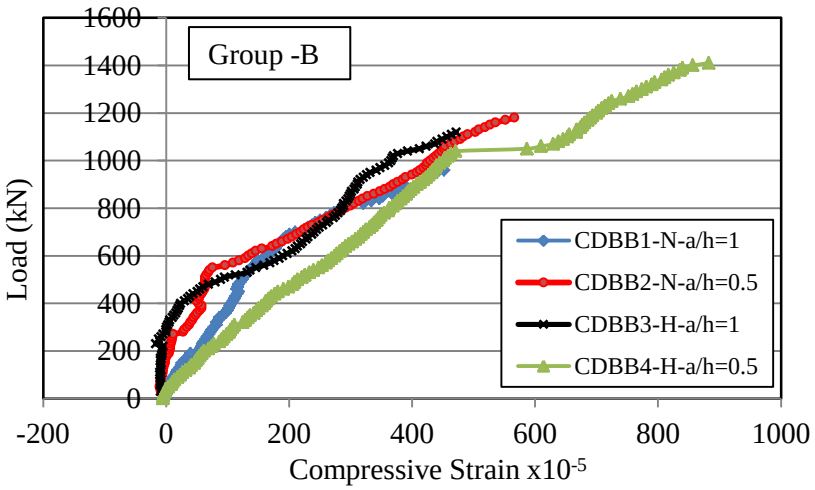

Figure 22. The concrete surface compressive strain in group (B)

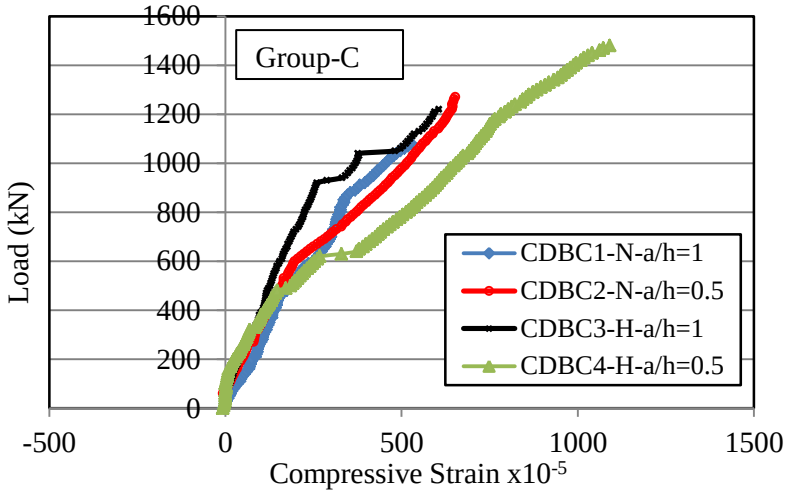

Figure 23. The concrete surface compressive strain in group (C)

15. Conclusions

The behavior of 12 reinforced SCC continuous deep beams have been studied, the major conclusions from the experimental tests of current work are summarized.

1- The ultimate failure load (P_{ult}) increases significantly as the ratio of shear span to overall depth ratio (a/h) decreases. It was found that when the ratio of shear span to overall depth ratio decreases from 1.0 to 0.5, the percentages of increase in the failure load by about (25.2% in average) and the first cracking load (P_{cr}) increases by about (29.4 % in average)

2- All tested SCC continuous deep beams were failed by shear. The shear failure took place by diagonal splitting mode for all tested beams.

3- Both, the ultimate load and first cracking load were improved by increasing the compressive strength of concrete from (33.81 to 68.33) MPa. Beams with high concrete compressive strength exhibits a noticeable enhancement in the ultimate load while a beam cast in normal SCC shows an improvement in cracking load only.

4- It was found that shear span to overall depth ratio (a/h) effects the load carrying capacity of beams such that a decrease of 50 % in that ratio from 1 to 0.5, the cracking load (P_{cr}) and ultimate load (P_{ult}) increase by average ratios of 29.35% and 25.15% respectively.

5- The load- mid span deflection curves appeared to be strongly dependent on the a/h ratio, magnitude and arrangement of web reinforcement. The deflection values of HSCC beams are always less than deflection values of NSCC beams for all stages of loading.

6- Increasing the magnitude of (ρv) by 80% (from 0.25% to 0.45%) that is (ρv_{min} & ρv_{max}) results in a better increase in the shear capacity of both NSCC & HSCC deep beam having (a/h) ratio of 1.0 (enhancement reached to18.56% and 23.1% respectively) while in case of (a/h) ratio of 0.5, it seems that deep beams cast in NSCC show good enhancement in ultimate load capacity (by 14.53%) while only

14.91% enhancement was noticed in beams cast in HSCC for the same (a/h) ratio of (0.5).

16. References

1. Ashour, A. E, and Morley, C. T. (1996). "*Effectiveness Factor of Concrete in Continuous Deep Beams*", Journal of Structural Engineering / February 1996.122:169-178.
2. Beshara F.B.A., Shaaban I.G., and Mustafa T.S, 2013 "*Behavior and Analysis of Reinforced Concrete Continuous Deep Beams*", 12th Arab Structural Engineering Conference, Tripoli, Libya**.**
3. B.Singh et.al (2006). "*Design Of A Continuous Deep Beam Using The Strut and Tie Method*", Asian Journal of Civil Engineering (Building and Housing) Vol. 7, No. 5,2006,461-477pp**.**
4. Kaszynska,M., 2004, "*Application of Self-compacting Concrete for the Repair of Concrete Structures*". M.Sc. Thesis, Department of Civil Engineering, Technical University of Szczecin,128 PP **.**
5. Subedi, N. K., Vardy, A. E., and Kubota, N., 1986, "*Reinforced Concrete Deep Beams- Some Test Results*", Magazine of Concrete Research, Vol. 38, No. 137, December, pp. 206-218 **.**
6. Ali, A.F., and Noori, A.N., 2017, "*Effect of Web Reinforcement on Self-Compacting Reinforced Concrete Continuous Deep Beams*", Journal of Engineering and Sustainable Development, Vol. 22, July, 211 PP.
7. ACI Committee 363, "*State-of-the-Art Report on High-Strength Concrete (ACI 363R-92)*", American Concrete Institute, Farmington Hills, Michigan, 1992, 55 pp**.**
8. ACI Commitee 318, "*Building Code Requirements for Structural Concrete, (ACI318M-11) and commentary (318R-11)*", American Concrete Institute, Farmington Hills, Michigan, USA, 2011, 503 pp**.**
9. IQS No. 5/1984, "*Portland Cement*", Central Agency for Standardization and Quality Control, Planning Council, Baghdad, Iraq.
10. IQS No. 45/1984, "*Aggregate from Natural Sources for Concrete*", Central Agency for Standardization and Quality Control, Planning Council, Baghdad, Iraq.
11. EFNARC: European Federation Dedicated to Specialist Construction Chemicals and Concrete Systems, "*Specifications and Guidelines for Self-Compacting Concrete*", Association House, 99 West Street, Farnham, Surrey, U.K., 2002, February, 32 pp**.**
12. Model Sika Fume-HR, "*Concrete Additives*", Sika Egypt for Construction Chemicals, Egypt, www.sika.com.eg**.**
13. ASTM Designation C370-05a, 2005, "*Standard Specification for Testing Method and Definitions for Mechanical Testing of Steel Products*", 2005 Annual Book of ASTM Standards, American Society for Testing and Material, Philadelphia, Pennsylvania, Section 1, Vol. 1.01, pp. 248-287.
14. Emborg, M., 2000, "*Mixing and Transport*", Final Report of Task 8.1, Betongindustri AB, Brite EuRam, Sweden, 65 PP **.**

15. Al- Jabri, L.A., 2005, "*The Influences of Mineral Admixtures and Steel Fibers on the Fresh and Hardened Properties of SCC*", M.Sc. Thesis, Al-Mustansiriayah University, Baghdad, Iraq, 135 PP.
16. ACI Committee 237R, 2007, "*Self Consolidating Concrete*", Reported by ACI Committee 237(ACI 237R-07), Emerging Technology Series, April, 30 PP.